

Title	Semipolar $\{n\bar{n}\}01\}$ InGaN/GaN ridge quantum wells ( $n = 1 - 3$ ) fabricated by a regrowth technique
Author(s)	Funato, Mitsuru; Kotani, Teruhisa; Kondou, Takeshi; Kawakami, Yoichi
Citation	
Issue Date	2012-04
URL	<a href="http://hdl.handle.net/2433/155465">http://hdl.handle.net/2433/155465</a>
Right	© 2012 American Institute of Physics.
Type	Thesis or Dissertation
Textversion	publisher

## Semipolar {n01} InGaN/GaN ridge quantum wells (n=1–3) fabricated by a regrowth technique

Mitsuru Funato, Teruhisa Kotani, Takeshi Kondou, and Yoichi Kawakami

Citation: *Appl. Phys. Lett.* **100**, 162107 (2012); doi: 10.1063/1.4704779

View online: <http://dx.doi.org/10.1063/1.4704779>

View Table of Contents: <http://apl.aip.org/resource/1/APPLAB/v100/i16>

Published by the [American Institute of Physics](http://www.aip.org).

---

### Related Articles

The contribution of quantum confinement to optical anisotropy of a-plane Cd<sub>0.06</sub>Zn<sub>0.94</sub>O/ZnO quantum wells  
*Appl. Phys. Lett.* **100**, 171910 (2012)

Strain-induced composition limitation in nitrogen δ-doped (In,Ga)As/GaAs quantum wells  
*Appl. Phys. Lett.* **100**, 171906 (2012)

The consequences of high injected carrier densities on carrier localization and efficiency droop in InGaN/GaN quantum well structures  
*J. Appl. Phys.* **111**, 083512 (2012)

Experimental and theoretical analysis of the temperature dependence of the two-dimensional electron mobility in a strained Si quantum well  
*J. Appl. Phys.* **111**, 073715 (2012)

Observation of gate-controlled spin—orbit interaction using a ferromagnetic detector  
*J. Appl. Phys.* **111**, 07C317 (2012)

---

### Additional information on *Appl. Phys. Lett.*

Journal Homepage: <http://apl.aip.org/>

Journal Information: [http://apl.aip.org/about/about\\_the\\_journal](http://apl.aip.org/about/about_the_journal)

Top downloads: [http://apl.aip.org/features/most\\_downloaded](http://apl.aip.org/features/most_downloaded)

Information for Authors: <http://apl.aip.org/authors>

## ADVERTISEMENT



GET YOUR COPY TODAY >>

**FREE CD with 700  
Multiphysics Presentations**

COMSOL

## Semipolar $\{n\bar{n}01\}$ InGaN/GaN ridge quantum wells ( $n = 1-3$ ) fabricated by a regrowth technique

Mitsuru Funato,<sup>a)</sup> Teruhisa Kotani, Takeshi Kondou, and Yoichi Kawakami  
 Department of Electronic Science and Engineering, Kyoto University, Kyoto 615-8510, Japan

(Received 8 January 2012; accepted 2 April 2012; published online 19 April 2012)

Semipolar  $\{n\bar{n}01\}$  InGaN/GaN quantum wells (QWs) ( $n = 1-3$ ) are fabricated on top of GaN microstructures, which consist of semipolar  $\{1\bar{1}01\}$  facets. Semipolar planes are obtained via regrowth of three-dimensional structures on (0001) GaN templates under controlled growth conditions. Compared to QWs on  $\{1\bar{1}01\}$  facets,  $\{n\bar{n}01\}$  ridge QWs show an intense emission at  $\sim 440$  nm. Time resolved photoluminescence reveals that the radiative lifetime of excitons in  $\{n\bar{n}01\}$  InGaN ridge QWs at 13 K is 310 ps, which is comparable to that in  $\{1\bar{1}01\}$  QWs. The estimated internal quantum efficiency at room temperature is as high as 57%. © 2012 American Institute of Physics. [<http://dx.doi.org/10.1063/1.4704779>]

Semiconductor micro- and nanostructures may offer platforms for next generation light emitters. For example, site-controlled quantum dots,<sup>1</sup> stimulated emissions from pyramidal GaN cavities,<sup>2</sup> and multi-color emissions from InGaN/GaN nanocolumns<sup>3</sup> may pave the way toward novel functional optical devices. Furthermore, InGaN quantum wells (QWs) grown on semipolar planes of GaN three-dimensional microstructures exhibit a higher radiative recombination probability than those grown on the conventional (0001) plane due to the reduced polarization effect.<sup>4-6</sup> Light emitting diodes (LEDs) have been fabricated using such semipolar QWs.<sup>7-10</sup> Additionally, three-dimensional QWs are promising for multi-color emissions, including white, because the In composition and InGaN thickness are spatially distributed due to their structure.<sup>5,11</sup> Three-dimensional LEDs with multi-color emissions have already been demonstrated,<sup>8-10</sup> and a unique function, external control of the emission color, has been added.<sup>9</sup>

In this study, we demonstrate that semipolar  $\{n\bar{n}01\}$  InGaN/GaN QWs ( $n = 1-3$ ) can be fabricated on (0001) GaN templates by a regrowth technique under appropriate growth conditions. Electron microscopy and photoluminescence (PL) spectroscopy are used to investigate the structural and optical properties. The results indicate that the fabricated QWs possess superior properties as light emitters.

Samples were grown on sapphire (0001) substrates using low-pressure (300 Torr) metalorganic vapor phase epitaxy (MOVPE) without intentional doping. Initially,  $\sim 3$   $\mu\text{m}$  thick GaN layers were grown, and a mask material (100 nm thick SiO<sub>2</sub>) was subsequently deposited *ex situ* by plasma enhanced chemical vapor deposition. Mask stripes were formed along the  $[11\bar{2}0]$  direction using conventional photolithography. Typical dimensions of mask opening and mask region are 5  $\mu\text{m}$  and 5–10  $\mu\text{m}$ , respectively. Subsequent regrowth of GaN in ambient H<sub>2</sub> creates microstructures composed of  $\{1\bar{1}01\}$  facets, as shown in the scanning electron microscopy (SEM) image of Fig. 1(a). Hydrogen is a typical carrier gas for GaN MOVPE, whereas to promote In incorporation from the vapor phase to the solid phase, N<sub>2</sub> is usually used for InGaN MOVPE. It should be noted that N<sub>2</sub> hampers

adatom migration and may alter the regrowth characteristics. Therefore, the growth behaviors of GaN and InGaN in N<sub>2</sub> must be clarified to control the regrowth of InGaN/GaN QWs on GaN microstructures. For this, GaN microstructures were formed in H<sub>2</sub> as shown in Fig. 1(a), and GaN or InGaN was subsequently grown in N<sub>2</sub>. The thicknesses of GaN or InGaN should be 450–500 nm on a planar (0001) plane. Figures 1(b) to 1(d) show the results. GaN grown in N<sub>2</sub> [Fig. 1(b)] creates steep ridge structures on top of the pre-existing microstructures. The ridge structure consists of  $\{1\bar{1}01\}$ ,  $\{2\bar{2}01\}$ , and  $\{3\bar{3}01\}$  planes, as discussed below. In contrast, InGaN growth in N<sub>2</sub> [Fig. 1(c)] barely affects the triangular cross section, but a detailed assessment using magnified SEM images [Fig. 1(d)] shows that the InGaN growth rate along the  $[0001]$  direction increases from 200 nm near the bottom of the underneath GaN microstructure to 700 nm at the top. These observations suggest that both Ga and In atoms on the growth surface migrate from the bottom mask region toward the top of the microstructures, where Ga atoms have a negligible mobility and form ridge structures. Although the mechanism responsible for the differences between GaN and InGaN is currently unknown, it may be related to evaporation; In atoms that reach the top should immediately evaporate due to their high vapor pressure, and In evaporation may accompany Ga evaporation.

The phenomena revealed in Fig. 1 inspired us to fabricate InGaN/GaN QWs on steep semipolar ridges. (In this paper, QWs on steep semipolar ridges are referred to as ridge QWs, whereas QWs on pre-existing, wider  $\{1\bar{1}01\}$  GaN facets are referred to as facet QWs.) Such ridge QWs may provide several advantages in terms of light emitters. First, the highly three-dimensional structure should lead to better light extraction. Second, because the ridge size along the ridge slope is on the order of a few tens to hundreds of nanometers, the additional carrier/exciton confinement should occur in the corresponding direction. That is, ridge QWs can be a type of quantum wire with strong carrier/exciton spatial confinement. Furthermore, it is noteworthy that high performance green laser diodes have been fabricated on  $\{2\bar{2}01\}$  substrates.<sup>12</sup>

Five period InGaN/GaN QWs were fabricated on GaN microstructures formed in H<sub>2</sub>. The growth conditions of the QW realize  $\sim 15\%$  In composition and an InGaN thickness

<sup>a)</sup>Electronic mail: funato@kuee.kyoto-u.ac.jp.

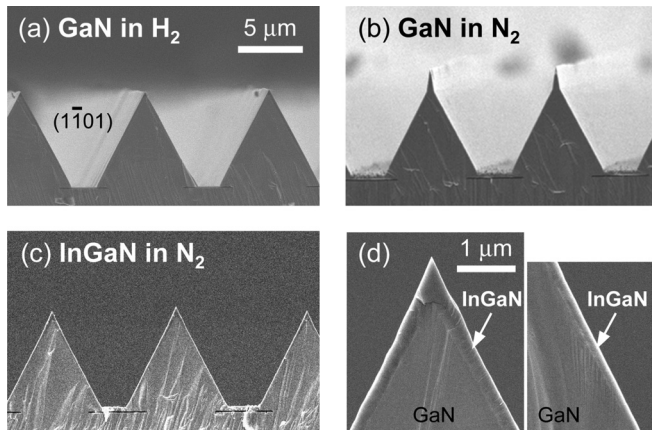


FIG. 1. (a) Cross-sectional SEM image of a GaN microstructure grown in  $H_2$ . On such a GaN microstructure, (b) GaN or (c) InGaN is grown in  $N_2$ . (d) Magnified SEM images of InGaN at the top (left) and near the bottom (right) of the GaN microstructure.

of 4 nm on the (0001) plane. Figure 2(a) shows an SEM image, which confirms the formation of ridge structures. Figure 2(b) is a scanning transmission electron microscopy (TEM) bright field (BF) image of the ridge region, which is denoted by a broken rectangle in Fig. 2(a). The image shows that wavy QWs form within the ridge. Considering the angles with respect to the [0001] direction, these wavy QWs consist of the  $\{1\bar{1}01\}$ ,  $\{2\bar{2}01\}$ , and  $\{3\bar{3}01\}$  semipolar planes, as designated by the broken lines in Fig. 2(b). The estimated well width is 4.2 nm. Additionally, QW fabrication is confirmed on the pre-existing  $\{1\bar{1}01\}$  facets with an estimated thickness of 2.8 nm (not shown). These well widths are consistent with Fig. 1 because In and Ga adatoms migrate toward the ridge. Figure 2(c) is a high resolution TEM image around the top of the third QW. The lattice image is distorted around the top of the third QW. The lattice image is distorted around the coalescence region of  $(n\bar{n}01)$  and  $(\bar{n}n01)$  ridge QWs, suggesting non-ideal coalescence. In fact, we experimentally confirmed that when the QW period is one, the emission from the ridge single QW, which forms a triangular cross section as shown in Fig. 2(b), is quite weak. Furthermore, its surface fluorescence image appears like a broken line. These findings suggest that the coalescence region of  $(n\bar{n}01)$  and  $(\bar{n}n01)$  ridge QWs has a marginal contribution to

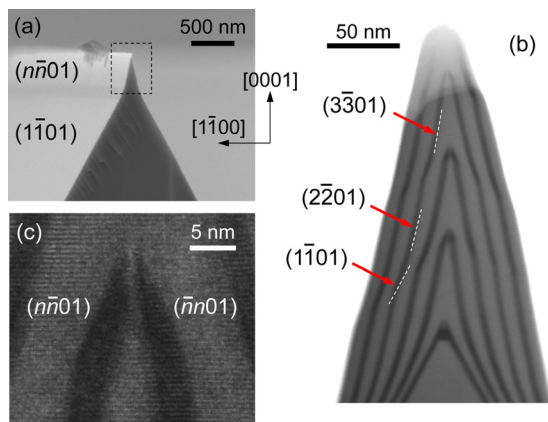


FIG. 2. (a) Cross-sectional SEM image of InGaN/GaN QW grown on a GaN microstructure. (b) Scanning TEM BF image of the ridge region designated by the broken rectangle in (a). (c) High resolution TEM image around the top of the third QW. TEM specimen is prepared by  $Ar^+$  milling, and the acceleration voltage is 200 KeV.

light emission, consistent with the high-resolution TEM observation [Fig. 2(c)]. In this respect, it is noteworthy that the emission properties of ridge “multiple” QWs shown below are governed by QWs except for the first QW.

Figure 3(a) shows a fluorescence microscopy image of five period InGaN/GaN ridge QWs acquired at the surface normal at room temperature. The emission from ridge QWs is much more intense than that from  $\{1\bar{1}01\}$  facet QWs, in spite of much smaller volume. At this stage, there are at least two possible reasons: a better internal quantum efficiency (IQE) or an improved light extraction efficiency. These reasons are discussed in detail below. Figure 3(b) displays top views of the cathodoluminescence (CL) intensity mappings monitored at various wavelengths. At shorter wavelengths, the emissions from both ridge QWs and the  $\{1\bar{1}01\}$  facet QWs are strong. In contrast, the PL of ridge QWs becomes predominant as the monitoring wavelength increases. These observations imply that the emission wavelengths differ between ridge and facet QWs. To directly confirm this assertion, CL spectra, which were locally acquired at a ridge and a facet, are compared in Fig. 3(c). As expected, the emission wavelength of ridge QWs is located at a longer wavelength.

Using the well widths determined by STEM and the emission wavelengths of the CL spectra, the deduced In compositions in ridge and facet QWs are 17% and 15%, respectively. Compared with the previous reports on faceted InGaN QWs,<sup>5,11</sup> the estimated spatial In distribution is small, which suggests that although InGaN and GaN exhibit quite different regrowth properties, as demonstrated in Figs. 1(b) and 1(c), In and Ga atoms migrate and evaporate quite similarly during InGaN regrowth. However, the growth mechanism behind it has yet to be clarified and is a subject of a future study.

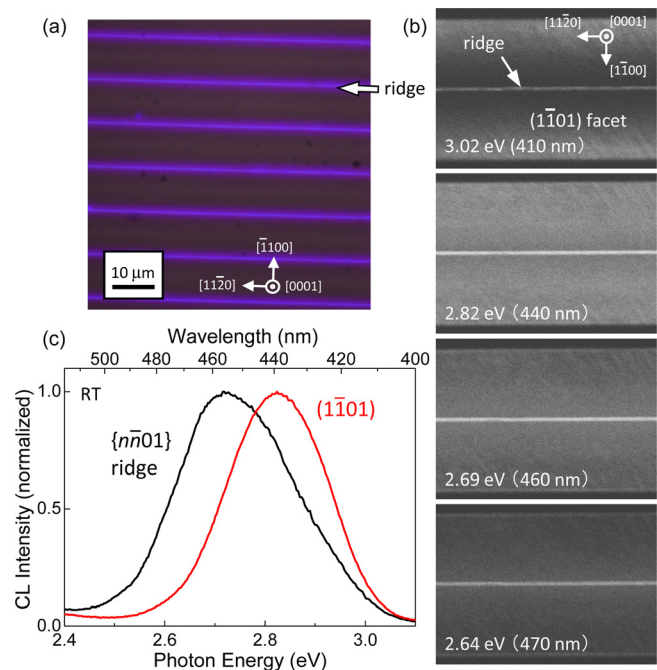


FIG. 3. (a) Fluorescence microscopy image of a ridge QW structure observed at the surface normal. (b) Top views of CL intensity distributions monitored at various emission wavelengths. (c) Normalized CL spectra acquired at a ridge QW and on a  $\{1\bar{1}01\}$  facet QW. All measurements are performed at room temperature.

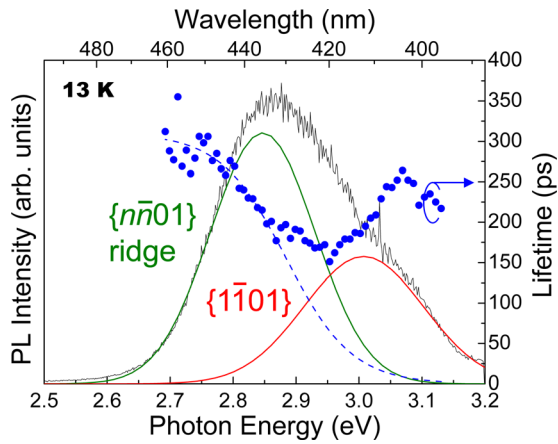


FIG. 4. Time-integrated PL spectrum and recombination lifetimes at 13 K. Two PL components within the PL spectrum emerge from the fit, representing those from the ridge and  $\{1\bar{1}01\}$  facet QWs. Weakly localized exciton model (broken line) provides a radiative lifetime of 310 ps for ridge QWs.

To assess the carrier recombination dynamics in ridge QWs, time-resolved PL (TRPL) was performed. The excitation source was a frequency doubled Ti:sapphire laser with a power density of  $0.12 \text{ nJ/cm}^2$ . The laser wavelength was 370 nm to selectively excite the QWs. PL was detected through a streak camera. Figure 4 shows a time-integrated PL spectrum and the recombination lifetimes acquired at 13 K. The PL spectrum was fitted with two Gaussian curves to separate the contribution of ridge QWs from that of the  $\{1\bar{1}01\}$  facet QWs. Figure 4 also plots the result of the fit. Comparing Figs. 3 and 4 reveals that the PL component at the longer wavelength is from ridge QWs. The estimated lifetimes plotted in Fig. 4 are affected solely by radiative recombination processes, particularly at low temperatures such as 13 K. Using a weakly localized exciton model,<sup>13</sup> the estimated radiative recombination lifetime in ridge QWs is 310 ps (dashed line in Fig. 4). It is noteworthy that 3 nm thick QWs on the conventional (0001) plane exhibit 5.2 ns at 2.9 eV. The reduced polarization effect in ridge QWs shortens the radiative lifetime and enhances its reciprocal; that is, the radiative recombination probability is enhanced. Although the radiative recombination lifetime for the  $\{1\bar{1}01\}$  facet QWs cannot be quantified due to the overlap of the PL spectra of ridge and facet QWs, it qualitatively appears to be on the same order of a few hundreds of ps.

To support the above arguments concerning the reduced polarization effect, the square overlap of electron and hole wavefunctions was calculated, assuming realistic quantum confinement with a finite barrier height. The square overlap is proportional to the radiative recombination probability. Table I summarizes the calculated results, where the In composition and well width were taken from the experimental results mentioned above. The square overlaps of the  $\{n\bar{n}01\}$  QWs ( $n = 1-3$ ) are on the same order as that of the  $\{1\bar{1}01\}$  QW, and are one order of magnitude greater than that of the (0001) QW. The calculated results qualitatively reproduce the trend of the experimentally determined radiative recombination probability, verifying the interpretation of the TRPL measurements. For quantitative fits between the calculation and the experiment, we have to take into account other factors such as in-plane carrier/exciton confinement, which

TABLE I. Calculated electric field (EF), transition energy at 0 K (TE), and square overlap of electron and hole wavefunctions (OL). The In composition and well width (WW) were taken from our experimental results.

Plane	$n$	In (%)	WW (nm)	EF (MV/cm)	TE (eV)	OL
(0001)		12	3.0	1.33	2.95	0.05
$\{n\bar{n}01\}$	1	17	4.2	0.51	2.84	0.23
	2			0.46	2.85	0.27
	3			0.35	2.87	0.39
$\{1\bar{1}01\}$		15	2.8	0.46	3.01	0.62

plays an important role in determining recombination processes.<sup>14,15</sup>

The high radiative recombination probability may provide a benefit of high IQE. To evaluate IQE, the PL temperature dependence was examined, using the same excitation setup as TRPL. Figure 5 shows the PL spectra acquired at 13 K and 300 K, and the intensity ratio between them well approximates IQE at 300 K. After decomposing the experimentally obtained PL spectra into two Gaussian components, which represent PL from ridge and facet QWs, such ratios were estimated for both the QWs. Figure 5 shows the fitting results. The estimated IQE for ridge QWs is 57%, while that for the  $\{1\bar{1}01\}$  facet QWs is 31%. Several mechanisms may explain the IQE difference: carrier transfer from the  $\{1\bar{1}01\}$  facets to  $\{n\bar{n}01\}$  ridges at elevated temperatures, larger non-radiative dislocation density in the  $\{1\bar{1}01\}$  facets due to bending of pre-existing threading dislocations parallel to the (0001) plane, and weaker carrier confinement in  $\{1\bar{1}01\}$  QWs both energetically and spatially. Although this study cannot reach a further conclusion, it should be noted that dislocations were not observed in ridge QWs using TEM. The improved IQE of ridge QWs may be one reason for the observed intense emission from ridge QWs [Figs. 3(a) and 3(b)], though contributions from other factors such as light extraction cannot be excluded.

In summary, we demonstrated that semipolar  $\{n\bar{n}01\}$  ( $n = 1-3$ ) QWs can be fabricated on the ridge of GaN microstructures by the regrowth technique.  $\text{N}_2$  carrier gas during the regrowth plays a principle role in forming such ridge

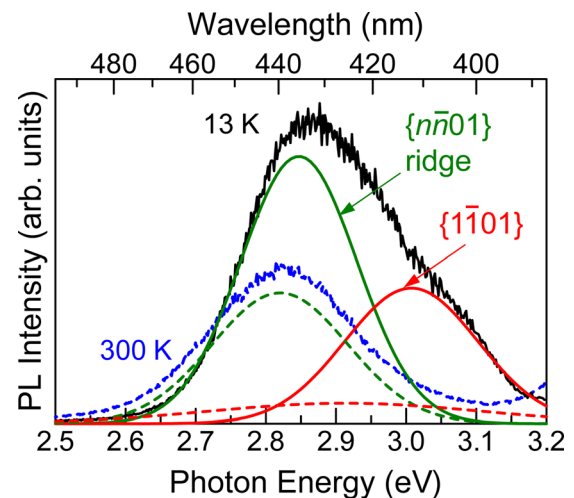


FIG. 5. PL spectra acquired at 13 K and 300 K. Solid and broken lines are for 13 K and 300 K, respectively. Tail observed at  $\sim 3.2$  eV is due to the excitation laser at 370 nm (3.35 eV).

structures. InGaN QWs fabricated on the  $\{n\bar{n}01\}$  ridge have a wider well width than  $\{1\bar{1}01\}$  facet QWs, and consequently, emit at a longer wavelength. The estimated radiative lifetime of the exciton in ridge QWs at 13 K is 310 ps, which is much faster than that of (0001) QWs and is comparable to that of the  $\{1\bar{1}01\}$  facet QWs. The fast radiative lifetime is attributed to the reduced piezoelectric effect. Due to this fast radiative lifetime, IQE at room temperature is as high as 57% for ridge QWs.

This work was partly supported by a Grant-in-Aid for Scientific Research and the Global Center-of-Excellence (G-COE) Programme of the Ministry of Education, Culture, Sports, Science, and Technology of Japan.

<sup>1</sup>K. Tachibana, T. Someya, S. Ishida, and Y. Arakawa, *Appl. Phys. Lett.* **76**, 3212 (2000).

<sup>2</sup>C.-M. Lai, H.-M. Wu, P.-C. Huang, S.-L. Wang, and L.-H. Peng, *Appl. Phys. Lett.* **90**, 141106 (2007).

<sup>3</sup>H. Sekiguchi, K. Kishino, and A. Kikuchi, *Appl. Phys. Lett.* **96**, 231104 (2010).

<sup>4</sup>K. Nishizuka, M. Funato, Y. Kawakami, Sg. Fujita, Y. Narukawa, and T. Mukai, *Appl. Phys. Lett.* **85**, 3122 (2004).

<sup>5</sup>K. Nishizuka, M. Funato, Y. Kawakami, Y. Narukawa, and T. Mukai, *Appl. Phys. Lett.* **87**, 231901 (2005).

<sup>6</sup>B. Neubert, P. Brückner, F. Habel, F. Scholz, T. Riemann, J. Christen, M. Beer, and J. Zweck, *Appl. Phys. Lett.* **87**, 182111 (2005).

<sup>7</sup>T. Wunderer, P. Brückner, B. Neubert, F. Scholz, M. Feneberg, F. Lipski, M. Schirra, and K. Thonke, *Appl. Phys. Lett.* **89**, 041121 (2006).

<sup>8</sup>M. Funato, T. Kondou, K. Hayashi, S. Nishiura, M. Ueda, Y. Kawakami, Y. Narukawa, and T. Mukai, *Appl. Phys. Express* **1**, 011106 (2008).

<sup>9</sup>M. Funato, K. Hayashi, M. Ueda, Y. Kawakami, Y. Narukawa, and T. Mukai, *Appl. Phys. Lett.* **93**, 021126 (2008).

<sup>10</sup>T. Wunderer, J. Wang, F. Lipski, S. Schwaiger, A. Chuvilin, U. Kaiser, S. Metzner, F. Bertram, J. Christen, S. S. Shirokov, A. E. Yunovich, and F. Scholz, *Phys. Status Solidi C* **7–8**, 2140 (2010).

<sup>11</sup>M. Funato, T. Kotani, T. Kondou, Y. Kawakami, Y. Narukawa, and T. Mukai, *Appl. Phys. Lett.* **88**, 261920 (2006).

<sup>12</sup>Y. Enya, Y. Yoshizumi, T. Kyono, K. Akita, M. Ueno, M. Adachi, T. Sumitomo, S. Tokuyama, T. Ikegami, K. Katayama, and T. Nakamura, *Appl. Phys. Express* **2**, 082101 (2009).

<sup>13</sup>C. Gourdon and P. Lavallard, *Phys. Status Solidi B* **153**, 641 (1989).

<sup>14</sup>Y. Narukawa, Y. Kawakami, M. Funato, Sz. Fujita, Sg. Fujita, and S. Nakamura, *Appl. Phys. Lett.* **70**, 981 (1996).

<sup>15</sup>M. Funato and Y. Kawakami, *J. Appl. Phys.* **103**, 093501 (2008).